Xiaohe Lai
Xin Deng
Cheng Chen
Chen Peng
Zixuan Li
Haoyan Chen

http://dx.doi.org/10.21278/brod74405

ISSN 0007-215X
eISSN 1845-5859

Study on the relationship between tsunami waves in dam break state and initial water levels

UDC 550.344.4:550.34.016
Original scientific paper

Summary

Tsunami wave characteristics are greatly influenced by the initial water level when they attack structures. In this study, experimental and numerical investigations were conducted to investigated the relationship between tsunami wave characteristics and initial water levels. Results showed that, the wave height, wave velocity, and Froude number increase with the increase of tsunami wave intensity; the time history of water levels were influenced by the different initial water level conditions; the analytical solution proposed by Chanson (2005) may be extended to wet-bed conditions (for initial water level < 0.36 tsunami bore height in our experimental set-up). Due to the limitations of experimental ranges in the laboratory, the validated numerical model can provide more results for wider experimental ranges for tsunami bore investigations. It was observed from numerical results that, tsunami bore height increases with the increase of reservoir water level; tsunami bore velocity decreases with the increased initial water level on the bed; as the initial water level on the bed gradually increases, the mean tsunami bore Froude number shows a downward trend.

Key words: *dam break wave, tsunami, initial water level*

1. Introduction

Tsunamis are caused by a series of unpredictable natural disasters, such as submarine volcano eruptions, submarine earthquakes, meteorite falls, and more [1]. Due to their wavelength being relatively long compared to the water depth [2], they can be regarded as shallow water waves. Under normal circumstances, tsunami waves have greater energy and faster propagation speed than ordinary sea surges and wind-induced waves. In deep water, the sudden displacement of the seabed terrain causes the water body to deviate from its equilibrium state. To counteract this deviation, the water surface generates oscillations and generates tsunami waves in the deep sea. These waves have a great amount of energy, and the energy loss of tsunami waves is inversely proportional to their wavelength, allowing them to

cross the entire ocean with minimal energy loss. As they propagate to the nearshore diving area, the wave peak increases and the wave steepness becomes steeper due to the shallower water depth, until it finally breaks.

According to the observations of significant tsunami events that have occurred since the 21st century, including the 2004 Indian Ocean tsunami [3], the 2011 Japan tsunami [4], the 2012 Haida Gwaii tsunami [5], and the 2022 Tonga tsunami [6], it has been found that tsunami waves can impact the coast within 5 to 20 minutes after an earthquake [7]. The submergence depth and run-up height of tsunami waves depend not only on the distance between the shoreline and the seismic source but also on the local seafloor topography and nearshore geomorphology. As tsunami waves gradually propagate towards the nearshore areas, their speed slows down and their height increases, ultimately engulfing the coastal regions in the form of broken waves and causing destructive damage to coastal structures [8].

Scholars have studied the causes of other hazardous weather such as tsunamis and their potential hazards in various ways. The similarity between typhoon-induced storm surges and tsunamis is analyzed by comparing the extreme weather conditions such as typhoon waves studied by Chen et al [9] using the SWAN model. For the numerical simulation of tsunami waves Xie et al [10] used the Navier-Stokes simulator - interFoam - to generate tsunami waves and investigated the rising mechanism of precursor low-pressure tsunami waves; Magdalena et al [11] used the staggered-grid finite-volume method to numerically analyze factors such as the amplitude of tsunami-related waves generated by underwater landslides. For physical modeling experiments Rajaie et al [12] investigated the effects of initial riverbed slope, initial impoundment depth, and static water level on the hydraulic characteristics of a dam failure tsunami wave generated by a rapid gate release through laboratory experiments. Von Haefen et al [13] calibrated a multiphase computational fluid dynamics numerical model through large-scale physical wave flume experiments, and proposed to predict land-based water flow characteristics by controlling the flow parameters to predict the empirical equations for overland flow characteristics. Yang et al. [14] conducted a study on the hydrodynamic interaction between dam-break waves and a circular pier. They conducted a series of experiments involving dam-break waves under both dry-bed and wet-bed conditions to observe and measure the evolution of wave front profiles. We refer to the experimental ideas and methods of scholars to verify the effect of initial water level on tsunami waves, generate dam breakers using the Dam-break Wave Generation System (DWSG), and compare them with the analytical solution provided by Chanson et al [15].

This paper aims to investigate the variation law of tsunami wave parameters through physical model tests and establish numerical simulation tests to obtain related tsunami wave parameters. We analyze the law and compare the results of the simulation tests with those of the physical model tests. In Section 2, we introduce the experimental site, instruments, and methods used in the study. Section 3 presents the experimental results, and Section 4 summarizes the conclusions drawn from our findings.

2. Experimental set-up

2.1. Facility

This experiment was conducted in the Hydraulic laboratory of the College of Civil Engineering, Fuzhou University, China. The experimental facility is shown in Fig. 1, which consists of a water storage reservoir, an experimental water tank, and a Dam-break Wave Generation System. The experimental water tank consists of a front discharge gate, a tsunami

wave propagation section, a slope, an adjustable baffle plate, and a rear energy dissipation and discharge tank.

The initial is an irregular polygon with the longest side of 12.3m, the widest side of 11.5m, a height of 0.8m, and a maximum working water depth of 0.7m. The storage capacity of the initial is 105m^3. The initial water level is controlled by an inlet valve and an outlet valve. By adjusting the flow of the inlet and outlet valves, the initial water level is maintained in dynamic balance. According to the experimental requirements, the storage initial water level is 0.7m, 0.6m, and 0.5m. The size of the tsunami wave generation tank is 16.5m × 1.5m × 0.8m (length × width × height). The water storage initial is connected to the tsunami wave front trough through a discharge gate. An energy dissipation pool, an adjustable water baffle, and a glass viewing window are installed at the end of the sink, and the adjustable water baffle is lifted during the experiment to stop the water flow from flowing down.

The Dam-break Wave Generation System (DWGS) used in this experiment is used to generate dam-break waves in the experimental tank to simulate tsunami waves. The DWGS consists of a gate control box, a computer operating system, and an outlet gate. Through the computer operating system, according to the set gate opening degree, a command is issued to the gate control box, which controls the hydraulic and pneumatic devices to quickly lift the outlet gate and release the water body. In the experimental tank, the strength of tsunami waves is controlled by three factors: (1) the opening degree of the gate; (2) the opening time of the gate; (3) the initial water level. When the gate is opened, the water flow at the top behind the gate is equivalent to a free-falling motion, while the water flow at the bottom moves horizontally [10]. When the outlet gate is opened for⩾4 seconds, a complete dam break tsunami wave can be formed. Therefore, the gate opening time is set to 5 seconds to ensure the formation of tsunami waves. The reservoir water level (RWL) is 0.70m, 0.60m, and 0.50m, and the gate opening (GO) is 0.35m.

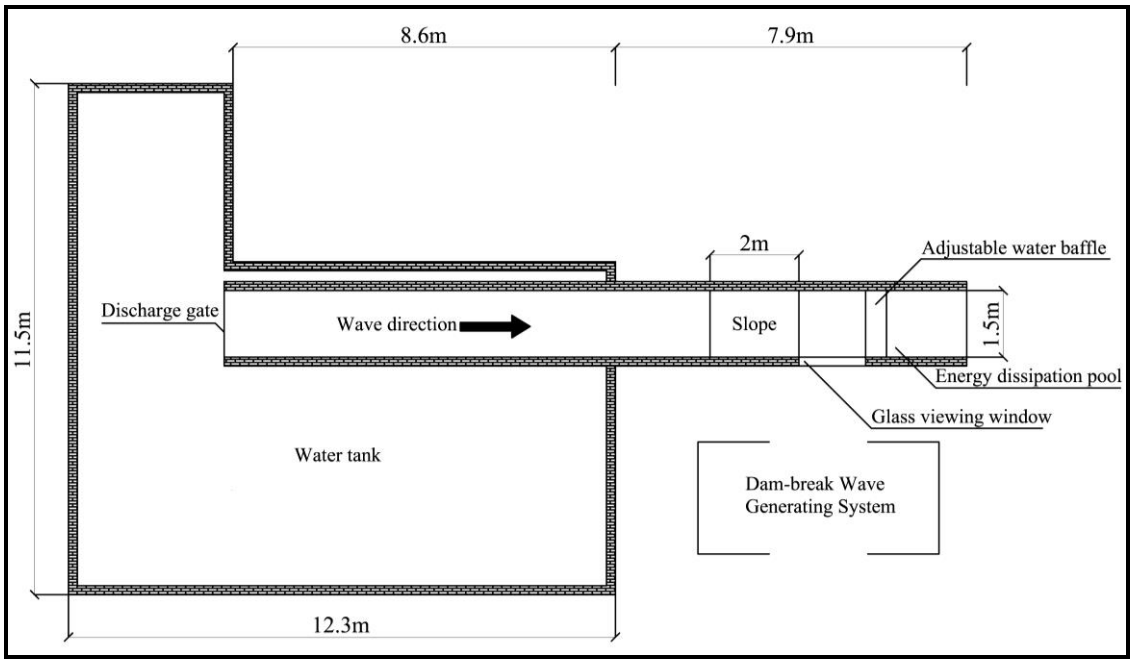

Fig. 1 Experimental facilities

2.2. Instruments

The tsunami wave height and velocity were measured by wave height gauges arranged with two wave height gauges mounted on the center flume of the tank (Fig. 5). The measurement range of the wave height gauges was 0 cm-70 cm, and the electrical signals were fed back to the computer through the water level changes. The wave height gauges were rate calibrated in the pre-test by placing them in a 70 cm measuring cylinder and calibrated by adding different water depths, resulting in a linear correlation between the water level and the electrical signal (shown in Fig. 2).

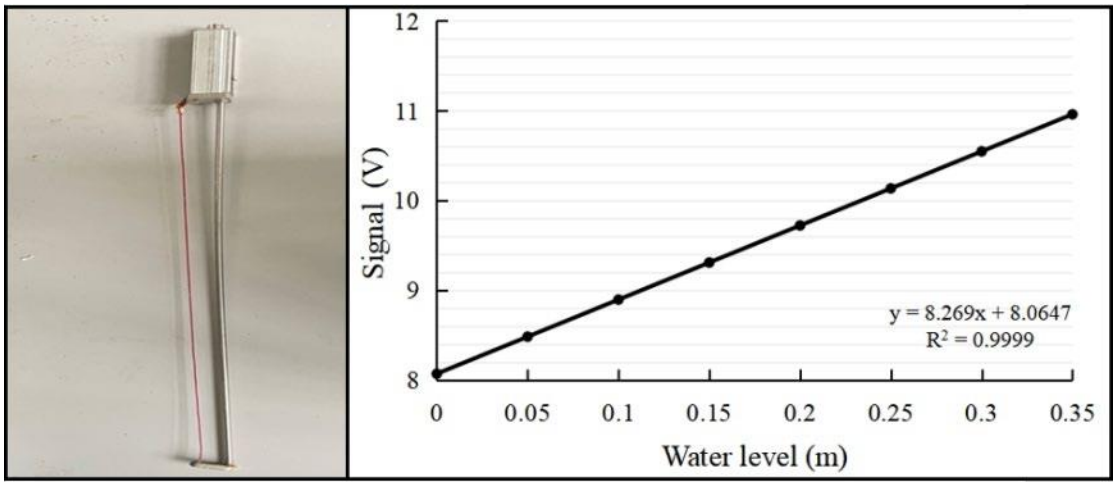

Fig. 2 Wave height gauge and its calibration

2.3. Wave height and velocity data processing

The method for measuring wave height is as follows: position wave height gauges 1# and 2# at distances of 10.60m and 9.60m, respectively, from the gate, with 1m between the two wave height gauges. Under various working conditions shown in Table 1, open the outlet gate, release the water behind, and generate a tsunami wave in a dam-breaking state. The wave height gauge records the entire process of water level change. When the water level recorded by wave height gauge 2# stabilizes, it is the height of the tsunami wave. Wave height gauge 1# is only used to calibrate the tsunami wave velocity measured by wave height gauge 2# because wave height gauge 1# is closer to the slope than wave height gauge 2# and is susceptible to interference from reflecting water, which results in inaccurate wave height data, and therefore the data collected by wave height gauge 1# is not used.

Table 1 List of various working conditions

RWL（m）	*GO*（m）	*IWL*（m）
0.70	0.35	0.00
		0.05
		0.10
0.60	0.35	0.00
		0.05
		0.10
0.50	0.35	0.00
		0.05
		0.10

A tsunami wave propagating in the flume first reaches wave height gauge 2#, which has a sudden change in its image, and then reaches wave height gauge 1#, which causes a sudden change in its image, and the difference in time between the sudden changes in the two wave height gauges is the time required for the tsunami wave to propagate between the wave height gauges (defined as Δt).The spacing of the wave height gauges is denoted by ΔL, and the average tsunami wave speed can be obtained from Eq. (1), which is regarded as an instantaneous speed in this paper because the spacing of the two wave height gauges in this experiment is 1 m, and the tsunami wave propagates in a very small amount of time between them.

The Froude number of tsunami waves can be obtained from wave height and wave velocity data according to Eq. (2) and compared with experimental results.

$$u_b = \Delta L / \Delta t \tag{1}$$

$$Fr_b = u_b / \sqrt{g h_b} \tag{2}$$

2.4. Numerical method

The layout of the experimental facility is shown in Fig. 3. Tsunami waves are simulated by quickly lifting the gate after a certain water level is filled in the rear initial. By changing the reservoir water level (RWL) and the initial water level (IWL), the wave height (h_b), wave velocity (u_b), and Froude number (Fr_b) which calculated using Eq. (1) and Eq. (2). The numerical flume model and the actual flume scale is 1:1 (as shown in Fig. 4), the calculation grid size is 0.01m×0.01m×0.01m, the numerical method adopts Moving and Simple Deforming Objects model, and by setting the speed of the gate moving up and down, to ensure that the GO is 0.35 at the same time, the gate rises and falls at the same speed. The attributes of each part of the flume are set as follows: Wall for the flume sidewalls and the bottom of the flume; Symmetry for the boundary of the opening above the flume; Outflow for the drainage outlet; Fluid Region 1 for the initial bed depth; Specified pressure for the storage reservoir; and Fluid Region 2 for the water level in the reservoir.

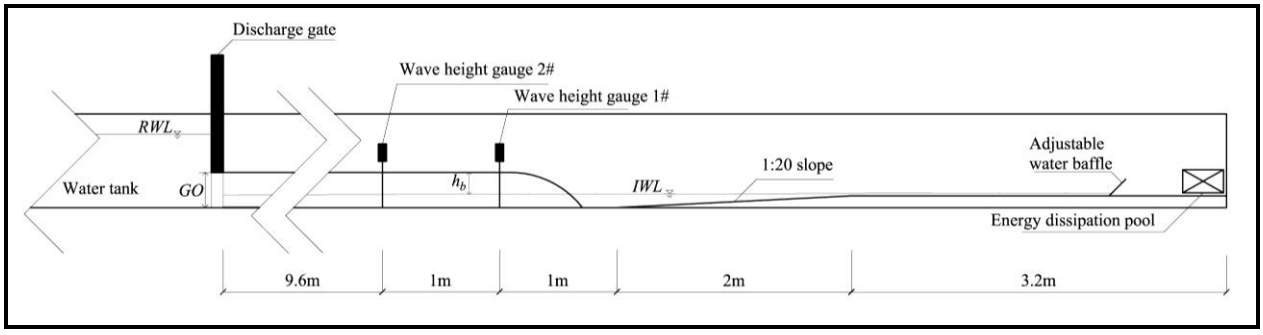

Fig. 3 Experiment layout diagram

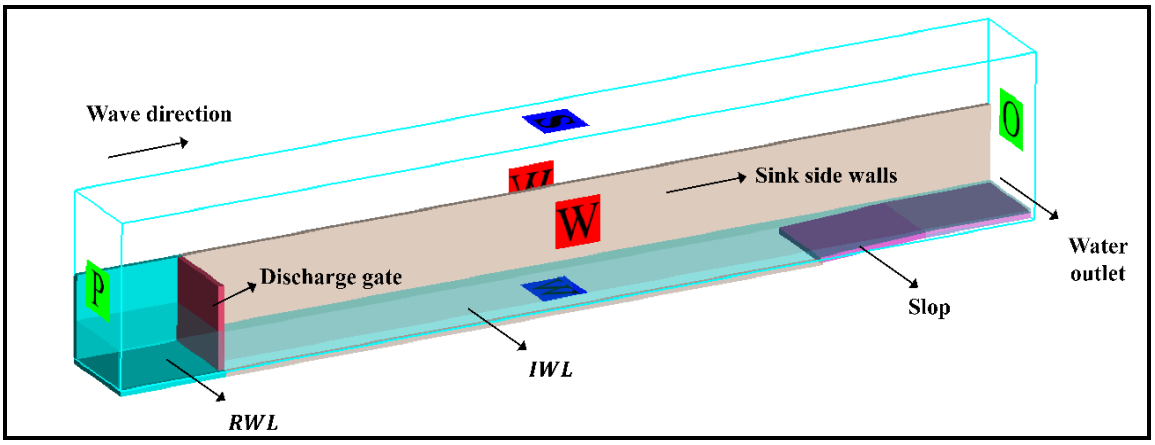

Fig. 4. Schematic diagram of numerical model water tank

3. Results and Discussion

3.1. Physical experiment results

3.1.1. Tsunami wave characteristics

As shown in Fig. 3 and Fig. 5, measurements were made using wave height gauges 1# and 2#, and the relevant of the tsunami wave were calculated. Table 2 shows the wave height (h_b), wave velocity (u_b), and Froude number (Fr_b), where Fr_b is calculated using Eq. (1).

From the table, under the same initial water level and the same gate opening, the wave velocity increases with the increase of the *IWL*, but the wave height and Froude number gradually decrease; Under the same gate opening and initial water level, as initial water level gradually increases, the wave velocity, wave height, and Froude number all increase.

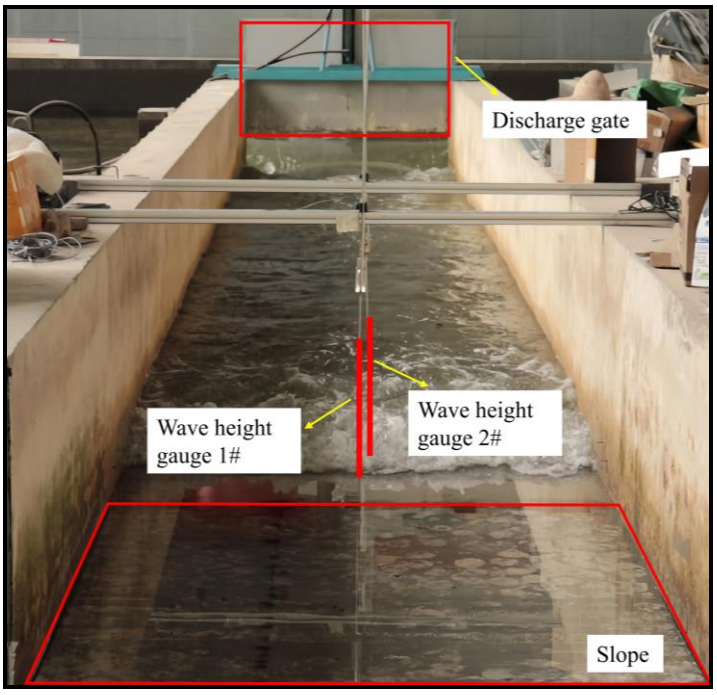

Fig. 5 *IWL* = 0.05m, *RWL* = 0.5m field test chart

Table 2 Table of Tsunami Wave under Various Operating Conditions (GO =0.35m)

IWL (m)	RWL (m)	u_b (m/s)	h_b (m)	Fr_b
0.00	0.70	4.69	0.27	2.9
	0.60	3.56	0.24	2.3
	0.50	3.70	0.23	2.5
0.05	0.70	2.85	0.21	1.8
	0.60	2.79	0.25	1.6
	0.50	2.38	0.21	1.5
0.10	0.70	2.37	0.28	1.2
	0.60	2.71	0.26	1.5
	0.50	2.29	0.23	1.3

3.1.2. The effect of initial water level on tsunami waves

Fig. 6 shows the water level duration curve measured by wave height gauge 2# under different initial water level on the bed surface. As shown in the figure, the steepness of the curve increases from 1s to 2s and then decreases from 2s to 6s. When $IWL = 0.00$ m, the water level duration curve needs to undergo more severe oscillations before reaching stability. when the initial water level is gradually increased, the water level duration curve shows a more pronounced variation, as can be seen in Fig.6 (a), (b) and (c).

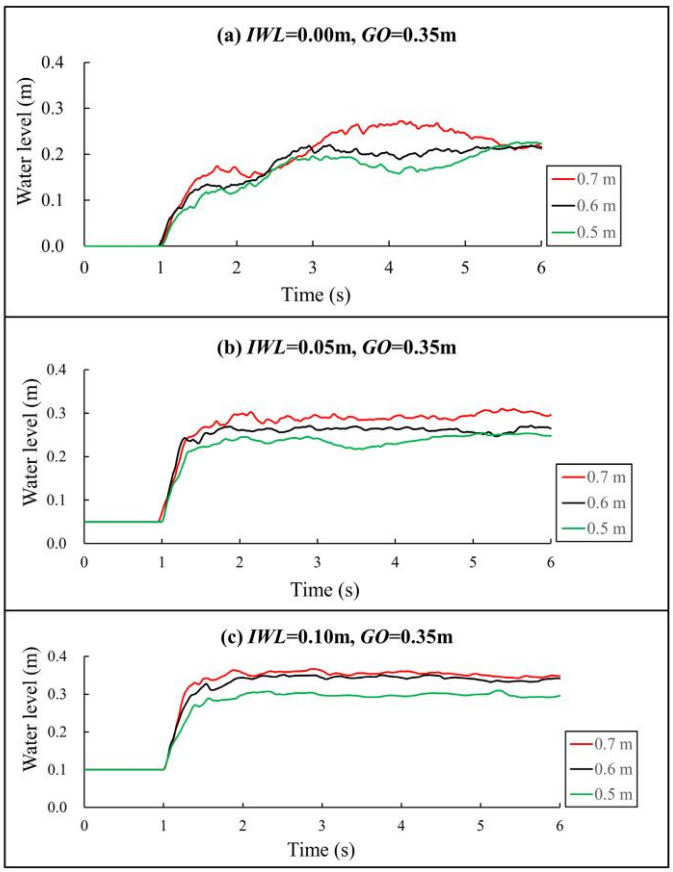

Fig. 6 Water level duration curve under different initial water level conditions on the bed surface (a. IWL =0.00m, GO =0.35m. b. IWL =0.05m, GO =0.35m. c. IWL =0.10m, GO =0.35m.)

3.1.3. Comparison between Tsunami Wave profile and Chanson's Analytical Solution

In the study of Chanson [15], an analytical solution for dam break waves was proposed, which is highly consistent with the on-site observation results of the 2014 Indian Ocean tsunami. The dam-break flow can be used to simulate tsunami waves, and the two have similar characteristics. Fig. 7 shows a comparison of the tsunami wave waveforms in 9 different dam failure states in this experiment with the analytical solution proposed by Chanson [15]. In Fig. 7, the horizontal axis represents the distance from the foot of the tsunami wave, while the vertical axis represents the height of the tsunami wave. From Fig. 7, it can be observed that the profiles of tsunami waves are different under different operating conditions in the near wave foot region, indicating that the initial water level (*IWL*) have a significant impact on the waveform of tsunami waves. The larger initial water level (*IWL*) results in the steeper tsunami wave front. It should be noted that, in our study, the analytical solution of the dam break wave profile obtained by Chanson [15] in Fig. 7 is mostly within the range of the results from *IWL* = 0.05 m, indicating that the analytical solution proposed by Chanson [15] may be extended to wet-bed conditions (for initial water level < 0.36 tsunami bore height in our experimental set-up).

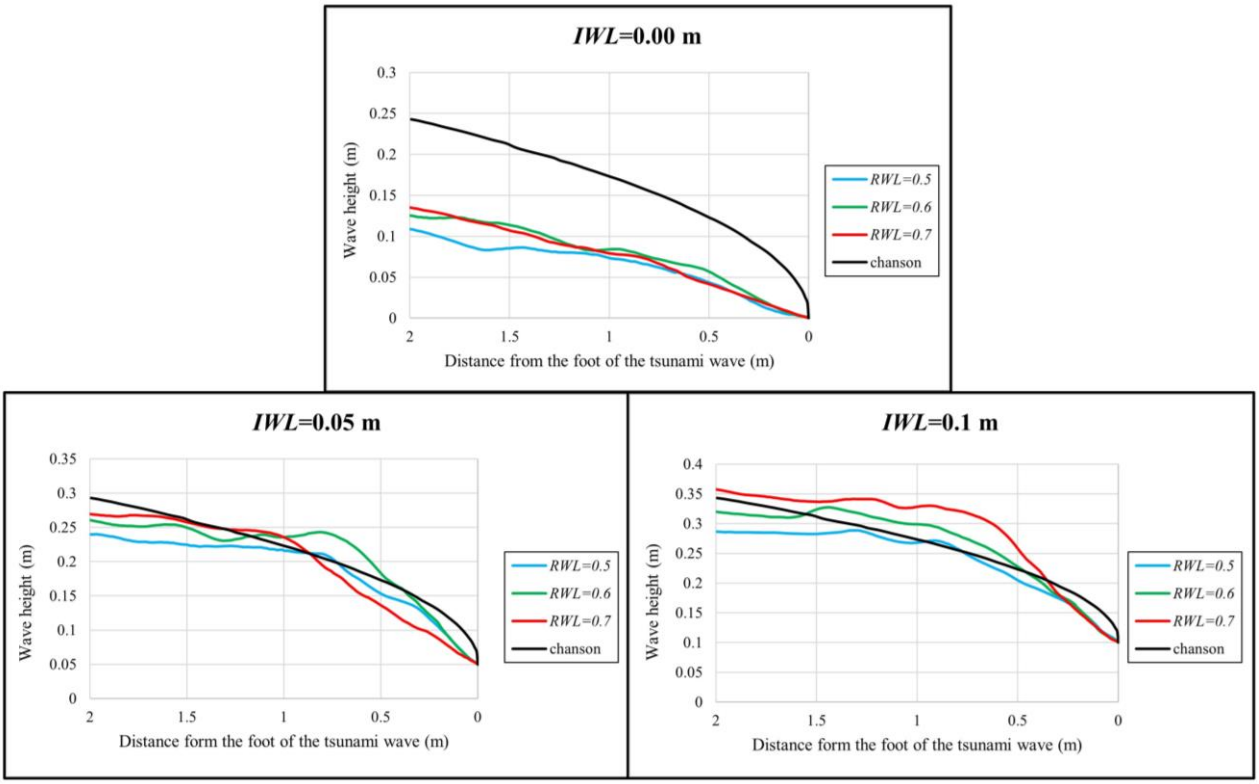

Fig. 7 Comparison between the tsunami wave waveform of this experiment and the results proposed by Chanson et al. [15]

3.2. Numerical simulation results

3.2.1. Numerical simulation process

After modeling and setting the relevant conditions in the numerical simulation model, the program operation was carried out to generate a dam break tsunami wave under the conditions of *RWL* =0.70m, *IWL* =0.05m and *GO* =0.35m. As shown in Fig. 8, the left side of X, Y, and Z represents the modeling coordinates, and the color block represents the free

surface elevation, which represents the water depth in gauges.

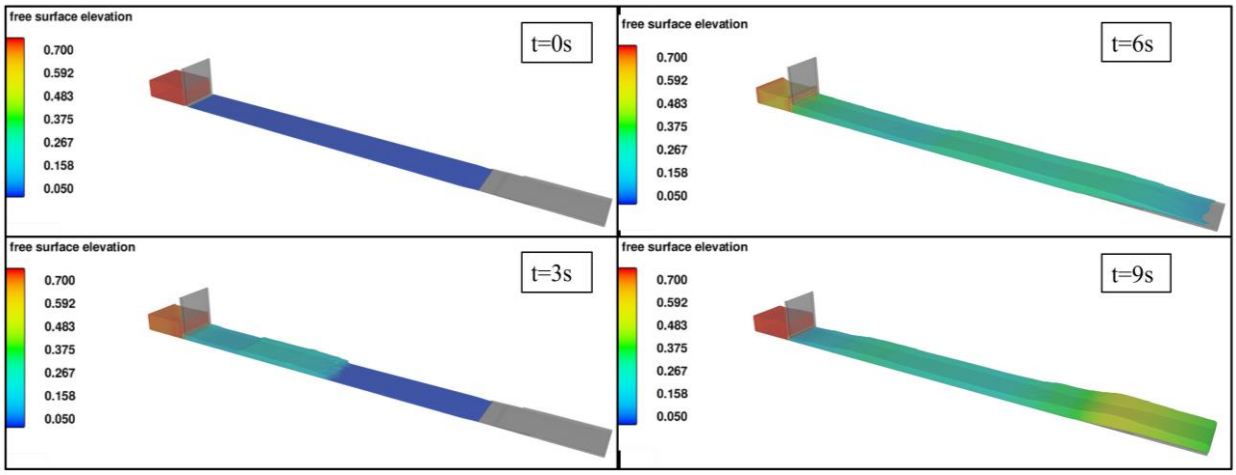

Fig. 8. The entire process of numerical simulation

At t=0s, the outlet gate is not opened, and the front and rear of the gate remain partially submerged at RWL=0.70m and IWL=0.05m, which is consistent with the actual experiment. At t=1s, the outlet gate rises upwards at a speed of 0.07m/s for a duration of 5s. As shown in the figure, at t=3s, the opening height of the outlet gate is GO=0.35m, and the rear initial continues to discharge water, generating a dam-breaking state of water flow and simulating tsunami waves. At t=6s, the outlet gate closes downwards at a speed of 0.07m/s until t=9s, and the outlet gate is completely closed. The numerical simulation experiment is completed.

3.3. Model validation

The measurement point selected in the three-dimensional water tank is the same as the position of the wave height gauge 2# in the actual experiment, and the wave height (h_{bM}) and wave velocity (u_{bM}) are obtained through measurement, while the Froude number (Fr_{bM}) is also obtained. In 3D numerical watercolor, in addition to the 9 working conditions mentioned above, other working conditions are added as shown in Table 3.

Fig. 9 shows the water level duration curve for conditions 1 to 9 in a numerical water tank. Comparing Fig. 6 (a) with Fig. 9 (a), when IWL=0.00m, the actual water level duration curve generated by the experiment is more rounded and fuller, while the water level duration curve obtained by numerical water tank simulation is sharper. In Fig. 9 (a), t=6s later. Due to the presence of a slope in the sink, the water flows back, and the water level rises, which is the same as the actual situation of tsunami waves. Compared with Fig. 6 (b) and (c), the overall water level duration curve in Fig. 9 (b) and (c) is similar. However, during the water level rise stage, the numerical simulation results require a longer time from the rise stage to the stable stage, and the graph is smoother. However, in actual experiments, the time required for the water level to rise to stability is shorter, and the graph slope is larger. It is believed that the numerically generated tsunami wave is consistent with the actual tsunami wave process. The water level duration curve under other working conditions is shown in Fig. 10.

Table 3 Summary of design conditions for 3D Numerical Flume

Conditions	*IWL* （m）	*RWL* （m）	*GO* （m）
1	0.00	0.70	0.35
2	0.00	0.60	0.35
3	0.00	0.50	0.35
4	0.05	0.70	0.35
5	0.05	0.60	0.35
6	0.05	0.50	0.35
7	0.10	0.70	0.35
8	0.10	0.60	0.35
9	0.10	0.50	0.35
10	0.15	0.70	0.35
11	0.15	0.60	0.35
12	0.15	0.50	0.35
13	0.20	0.70	0.35
14	0.20	0.60	0.35
15	0.20	0.50	0.35
16	0.25	0.70	0.35
17	0.25	0.60	0.35
18	0.25	0.50	0.35
19	0.30	0.70	0.35
20	0.30	0.60	0.35
21	0.30	0.50	0.35

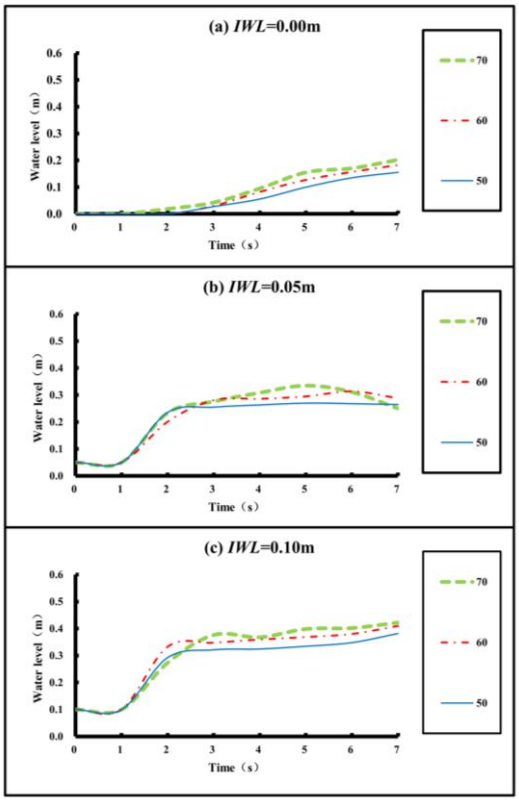

Fig. 9 Numerical water tank simulation of water level duration curves for operating conditions 1-9

To further determine the reliability of the tsunami waves generated by numerical simulation, the simulated tsunami waves h_{bM} and u_{bM} were compared with the measured tsunami waves h_b and u_b in the experiments. The comparison results are shown in Fig. 11, where the data points obtained from both wave height and wave velocity numerical simulations can be uniformly distributed on both sides of a 1:1 straight line, with an error of no more than 10%.

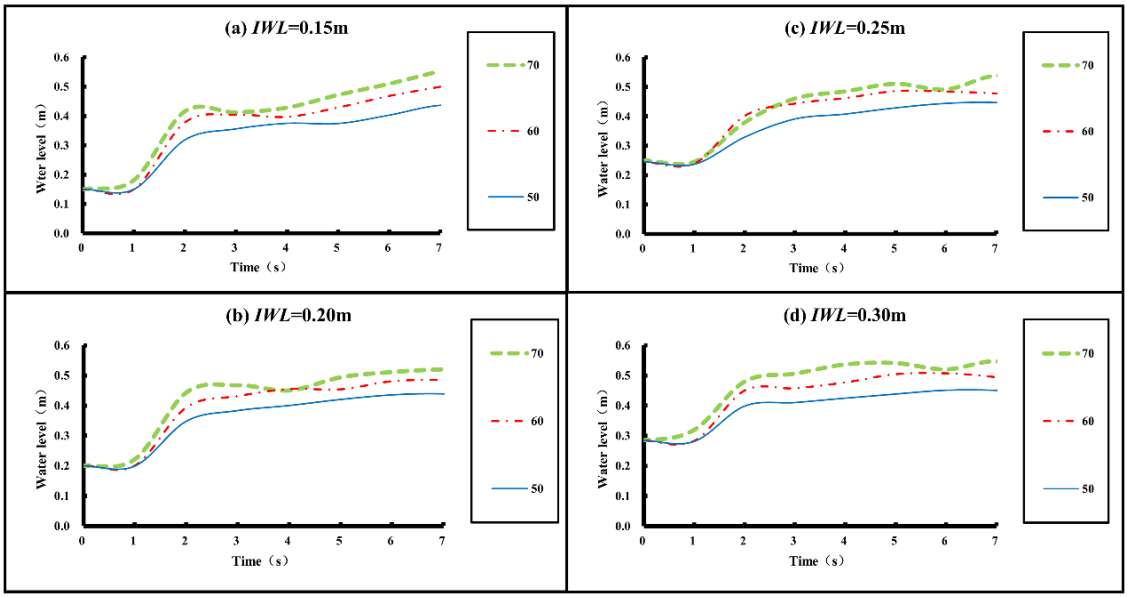

Fig. 10 Numerical simulation of water level duration curve for working conditions 10 -21

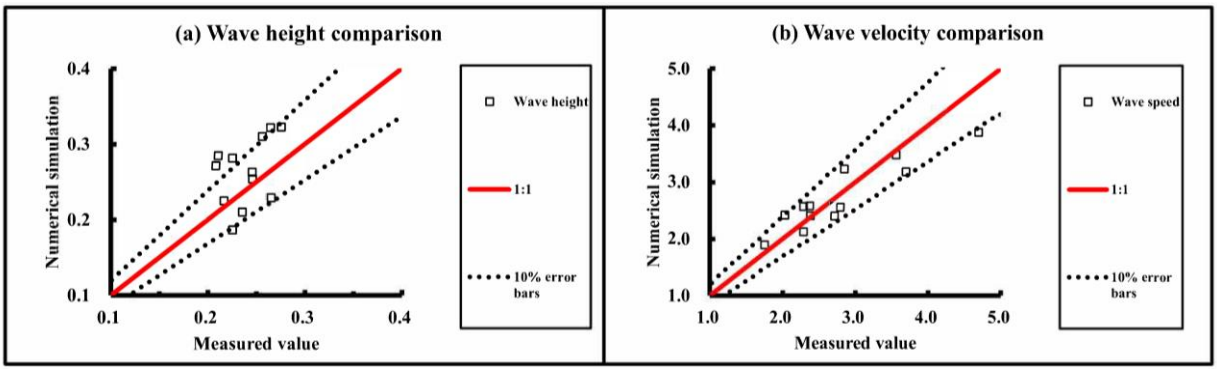

Fig. 11 Comparison of Numerical Simulation Tsunami Wave and Experimental Tsunami Wave under Conditions 1 to 12

3.4. Preliminary study on the laws of wave height, wave velocity, and Froude number in numerical simulation models

Simulate tsunami waves using a 3D numerical water tank and measure the tsunami waves generated under 9 set operating conditions, obtaining the tsunami wave height (h_{bM}), wave velocity (u_{bM}), and Froude number (Fr_{bM}), respectively. Table 4 shows the tsunami wave characteristic obtained from numerical simulation experiments under various operating conditions. As shown in Table 3.3, when IWL is a constant value, as RWL gradually increases, that is, the intensity of the tsunami wave increases, corresponding to h_{bM} , u_{bM} , and Fr_{bM} all gradually increase, and regardless of whether IWL is 0.05m or 0.10m, this

pattern is the same. This conclusion is the same as the conclusion obtained in section 3.1.

Fig. 12 (a) shows the relationship between RWL and h_{bM} under different IWL, it is believed that regardless of the type of IWL, h_{bM} increases with the increase of RWL. Fig. 12 (b) shows the relationship between RWL and u_{bM} under different IWL, it can be seen that u_{bM} increases with the increase of RWL. When RWL is a constant value, u_{bM} decreases as IWL increases. Fig. 12 (c) shows the relationship between Fr_{bM}, IWL, and RWL. When IWL=0.00m, the trend of Fr_{bM} increasing with RWL is relatively slow, while in other IWL under certain conditions, this change is more pronounced. Fig. 12 (d) shows the relationship between the average of Fr_{bM} and IWL. As IWL gradually increases, the average of Fr_{bM} shows a downward trend.

Table 4 Tsunami Wave Characteristic under Different Operating Conditions

Conditions	h_{bM} （m）	u_{bM} （m/s）	Fr_{bM}
1	0.23	3.86	0.86
2	0.21	3.48	0.84
3	0.19	3.18	0.87
4	0.28	3.23	0.58
5	0.26	2.56	0.50
6	0.27	2.41	0.45
7	0.32	2.58	0.41
8	0.31	2.40	0.40
9	0.28	2.13	0.39
10	0.32	2.57	0.41
11	0.25	2.41	0.48
12	0.23	1.89	0.43
13	0.29	2.42	0.42
14	0.26	1.95	0.39
15	0.22	1.48	0.34
16	0.26	2.34	0.46
17	0.24	1.57	0.34
18	0.18	0.95	0.27
19	0.24	2.25	0.48
20	0.20	1.08	0.27
21	0.14	0.80	0.30

4. Limitations of this study

1. In this paper, due to the limitations of the test equipment and other factors, failed to take into account the impact of bed friction, to be perfected after the theory and equipment conditions will be bed friction factors to be taken into account.
2. The effect of gate rise rate on tsunami wave formation was not considered in the paper and will be discussed in a subsequent study.
3. Due to the limitation of the experimental facilities, in this paper, the Froude number using distance-averaged velocity and instantaneous wave height at a fixed site may

not fully adhere to rigorous standards.

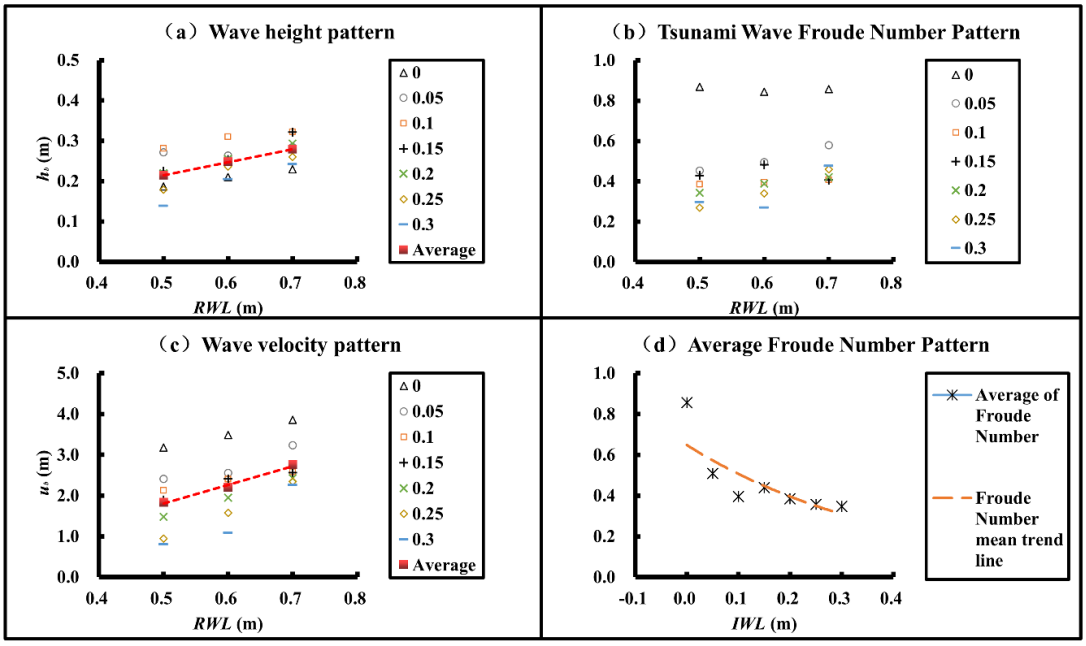

Fig. 12 Numerical simulation experiment tsunami wave patterns

5. Conclusions

This study investigated the effect of initial water level on dam break liked tsunami wave. Through physical experiments, the wave height (h_b) and wave velocity (u_b) of the tsunami wave are obtained using a wave height gauge, and the Froude Number is calculated. The results obtained through physical and numerical modeling experiments are as follows:

1. Under the same gate opening degree (GO) and initial water level (IWL), the wave height, wave velocity, and Froude number increase with the increase of tsunami wave intensity (the tsunami wave intensity in this paper refers to the reservoir water level, and the deeper the reservoir water level, the greater the intensity of the tsunami wave.).
2. Based on the data measured by a wave height gauge, the time history of water level under different initial water level conditions are plotted. It is observed that when IWL =0.00m, the line oscillates violently. When $IWL \neq$0.00m, the water level oscillation is small and reaches the stable value. The tsunami wave profiles obtained from the experimental measurements were compared with the dam-break waves proposed by Chanson et al. 2005, and the simulated dam-break waves from this experiment were considered reasonable.
3. Comparing the water level duration curves for different conditions in the numerical experiment with the measured data, it is believed that the water level duration curve generated by the experiment is more rounded and fuller, while the numerical water tank simulation results are sharper, and the time required for the water level to rise to stable is longer.
4. Tsunami wave Froude number does not have a fixed value and is a characteristic of tsunami wave motion over different beds. In this paper the tsunami wave Froude number ranges from 1.2-2.9, in other studies, Lukkunaprasit P et al. [16] found that

the tsunami wave Froude number varies from 2.4-3.0 when the tsunami wave travels on a very gentle slope of 0.5°, Matsutomi and Okamato [17] through experiments, the tsunami impacts on rectangular building with vertical wall structure has a tsunami wave Froude number in the range of 0.7-2.0, it can be seen that the tsunami wave Froude number in this paper is reasonable.

5. Comparing the results of h_{bM} and u_{bM} with the actual experimental measurements of h_b and u_b, The error of the obtained results is around ten percent, and the numerical simulation results are considered to be highly reliable.
6. Within a certain rage of IWL, h_{bM} increases with the increase of RWL; When RWL is a constant value, u_{bM} decreases as IWL increases; As the IWL gradually increases, the mean Fr_{bM} shows a downward trend.

Acknowledgments

The work was financially supported by the National Natural Science Foundation of China (Grant No. 51809047); the National Natural Science Foundation of China (Grant No. U22A20585); Fujian Provincial Natural Science Foundation (Grant No. 2019J05029).

REFERENCES

[1] Al-Faesly, T., Palermo, D., Nistor, I., Cornett, A., 2012. Experimental modeling of extreme hydrodynamic forces on structural models. *International Journal of Protective Structures*, 3(4), 477-506. https://doi.org/10.1260/2041-4196.3.4.477

[2] Thusyanthan, N., I., Madabhushi, S., 2008. Tsunami Wave Loading on Coastal Houses: A Model Approach. *New civil engineer international*, 161(2), 77-86. https://doi.org/10.1680/cien.2008.161.2.77

[3] Kurian, N.P., Baba, M., Rajith, K., Nirupama, N., Murty, T.S., 2006. Analysis of the Tsunami of December 26, 2004, on the Kerala Coast of India—Part I: Amplitudes. *Marine Geodesy*, 29(4), 265-270. https://doi.org/10.1080/01490410601008861

[4] Sato, S., 2015. Characteristics of the 2011 Tohoku Tsunami and introduction of two level tsunamis for tsunami disaster mitigation. *Proceedings of the Japan Academy. Series B, Physical and Biological Sciences*, 91(6), 262-72. https://doi.org/10.2183/pjab.91.262

[5] Sheehan, A. F., Gusman, A. R., Heidarzadeh, M., Satake, K., 2015, Array Observations of the 2012 Haida Gwaii Tsunami Using Cascadia Initiative Absolute and Differential Seafloor Pressure Gauges. *Seismological Research Letters*, 86(5). 1278-1286. https://doi.org/10.1785/0220150108

[6] Carvajal, M., Sepúlveda, I., Gubler, A., Garreaud, R., 2022. Worldwide signature of the 2022 Tonga volcanic tsunami. *Geophysical Research Letters*, 49(6). https://doi.org/10.1029/2022GL098153

[7] An, C., 2021. Tsunamis and tsunami warning: Recent progress and future prospects. *Science China Earth Sciences*, 64(2), 191–204. https://doi.org/10.1007/s11430-020-9672-7

[8] Hasanpour, A., Istrati, D., Buckle, I., 2021. Coupled SPH-FEM Modeling of Tsunami-Borne Large Debris Flow and Impact on Coastal Structures. *Journal of marine and engineering*, 9(10), 1068. https://doi.org/10.3390/jmse9101068

[9] Chen, C., Peng, C., Xiao, H., Wang, T.Y., Wei, M. J., 2022. Numerical distribution simulation of typhoons' wave energy in the Taiwan Strait and its adjacent waters. *Brodogradnja*, 73(4), 39-52. http://dx.doi.org/10.21278/brod73403

[10] Xie, P., W., Du, Y., 2023. Tsunami wave generation in Navier-Stokes solver and the effect of leading trough on wave run-up. *Coastal engineering*, 182. https://doi.org/10.1016/j.coastaleng.2023.104293

[11] Magdalena, I., Firdaus, K., Jayadi, D., 2022. Analytical and numerical studies for wave generated by submarine landslide, *Alexandria engineering journal*, 61(9), 7303-7313. https://doi.org/10.1016/j.aej.2021.12.069

[12] Rajaie, M., Azimi, A., Nistor, I., Rennie, C.,2022. Experimental Investigations of the Impact of Tsunami-Like Hydraulic Bores on a Square Vertical Structure. *Journal of Waterway, Port, Coastal, and Ocean Engineering*, 148 (3). https://doi.org/10.1061/(ASCE)HY.1943-7900.0001965

[13] von Haefen, H., Krautwald, C., Bihs, H., Goseberg, N., 2022. Dam-Break Waves' Hydrodynamics on Composite Bathymetry, *Frontiers in Built Environment*, 8. https://doi.org/10.3389/fbuil.2022.877378

[14] Yang, S., Tan, Z., Yang, W., Imani, H., Song, D., Luo, J., Zhang, J., 2022. Experimental study on hydrodynamic interaction between dam-break waves and circular pier. *Ocean Engineering*, 226, 113093. https://doi.org/10.1016/j.oceaneng.2022.113093

[15] Chanson, H., 2005. Analytical solution of dam break wave with flow resistance: application to tsunami surges. *31st IAHR Biennial Congress*, 137 (1), 3341-3353.

[16] Lukkunaprasit, P., Ruangrassamee, A., Thanasisathit, N., 2009. Tsunami loading on buildings with openings. *Science of Tsunami Hazards*, 28(5), 303-310.

[17] Matsutomi, H., Okamoto, K., 2010. Inundation flow velocity of tsunami on land. *Island Arc*, 19, 443-457. https://doi.org/10.1111/j.1440-1738.2010.00725.x

Submitted: 10.05.2023.
Accepted: 09.08.2023.

Xiaohe Lai, laixiaohe@fzu.edu.cn
Xin Deng, 707025863@qq.com
Cheng Chen*, chencheng_1117@163.com
Chen Peng, 1525246577@qq.com
Zixuan Li, 602658712@qq.com
Haoyan Chen, 543431935@qq.com
College of Civil Engineering, Fuzhou University, Fuzhou 350108, China